MANGANESE OXIDE NANOPARTICLES DERIVED USING *DRACOCEPHALUM MOLDAVICA* SEED MUCILAGE: AN EFFICIENT, BIOCOMPATIBLE, AND ENVIRONMENTALLY BENIGN ROUTE

Tuba [1,2], **Alina Sionkowska** [1,2]

[1] Laboratory for Biomaterials and Cosmetics, Faculty of Chemistry, Nicolaus Copernicus University in Toruń, Gagarina 7, 87-100 Toruń, Poland
[2] Institute of Advanced Studies, Nicolaus Copernicus University in Toruń, 87-100 Toruń, Poland

Email: tuba@doktorant.umk.pl, alinas@umk.pl

Abstract

Recently, biopolymers extracted from natural resources have shown remarkable potential for engineering nanomaterials, integrating the principle of green chemistry while reducing the traditional approaches-associated ecological footprints. In this study, bio-inspired fabrication of manganese oxide nanoparticles (MnO NPs) was achieved using *Dracocephalum moldavica* seed mucilage under mild reaction conditions. A comprehensive evaluation of their optical, surface chemical, structural, and morphological properties was performed. A preliminary criterion for the synthesis of NPs was assessed from an instantaneous color change from dark purple to blackish brown. The ultraviolet-visible (UV-vis) spectrum showed a distinct and well-defined surface plasmon resonance peak (SPR) at around 223 nm, while the functional groups of phytoconstituents acting as reducing and capping agents were identified using Fourier-transform infrared spectroscopy (FTIR). The X-ray diffraction (XRD) pattern confirmed characteristic peaks at 2θ values of 22.4, 37.12, and 65.9°, pointing towards the cubic structure of MnO NPs. Scanning electron microscopy (SEM) photographs demonstrated the roughly spherical morphology, while a particle size distribution histogram, generated using the ImageJ software, revealed an average diameter of 82.5 nm. The elemental mapping associated with the bio-produced NPs displayed the predominance of manganese (45.07%) and oxygen (41.87%), corresponding to a stoichiometric ratio close to 1:1. The outcomes support the suitability of *D. moldavica* seed mucilage as a template for biogenic nanomaterials, thereby paving the way for further advancement in green nanotechnology strategy.

Keywords: *Nanotechnology; phytoconstituents; Dracocephalum moldavica; mucilage; manganese oxide nanoparticles; comprehensive characterization*

[Engineering of Biomaterials 174 (2026) 17]

doi:10.34821/eng.biomat.174.2026.17

Submitted: 2026-09-10, Accepted: 2026-10-24, Published: 2026-11-16

Copyright © 2026 by the authors. Some rights reserved. Except otherwise noted, this work is licensed under **https://creativecommons.org/licenses/by/4.0**

Introduction

Among various multidisciplinary areas of applied sciences, nanotechnology has observed tremendous growth by enabling the engineering and utilization of very small nanoscale materials. At this scale range, the manufactured objects exhibit extraordinary capabilities and offer several advantages compared to their bulk counterparts [1]. For instance, owing to their miniature sizes and high surface-area-to-volume ratios, nanomaterials are considered indispensable in advanced technologies and fundamental research, thereby creating new opportunities across biomedical, environmental, energy, agricultural, and industrial sectors [2]. A great extent of research is conducted towards developing nanomaterials, especially nanoparticles, because of their easy preparation and facile surface functionalization. At present, numerous nanoparticles, including silver, gold, palladium, zinc oxide, manganese oxide (MnO), titanium dioxide (TiO_2), and alumina (Al_2O_3), have been fabricated in the fields of chemical, physical, and materials sciences [3]. Among these, MnO NPs are highly adaptable nanoplatforms due to their tunable morphologies/structures, excellent physicochemical properties, wide variety of oxidative states, environmental and ecological compatibility, and green character [4]. The unique characteristics have facilitated major applications in drug delivery systems, therapeutic formulations, nutritional supplements, biosensing, ion-exchange, adsorption, cosmetics, and textile industries [4,5].

Different strategies have been taken into consideration to produce MnO NPs, such as laser ablation, co-precipitation, electrodeposition, reduction-oxidation, sonochemical reduction, hydrothermal/solvothermal, sol-gel, and reflux methods [6-11]. Most of these approaches often rely on expensive equipment, toxic/hazardous reagents, high solvent consumption, and energy-intensive processes [12], hence creating concerns in line with the world's environmental objectives. These limitations make it significant to investigate environmentally preferable alternatives that prioritize sustainable exploitation as well as economic and environmental friendliness. Green synthesis, leveraging bio-ingredients, such as metabolites/phytoconstituents from various plant/microbial extracts, has drawn considerable attention for the generation of metal oxide NPs with varying shapes and sizes [13–16]. Existing literature confirmed the production of MnO NPs using *Syzygium aromaticum* flower buds, *Malpighia emarginata* and *Yucca gloriosa* leaves, *Tinospora cordifolia* stem, *Cydonia oblonga* seed mucilage, and *Trichoderma virens* strain EG92 [17–22]. Among the aforementioned methods, mucilage is attracting the vigil eye of researchers as a natural reducing-cum-capping agent besides its uses as a gelling agent, stabilizer, emulsifier, texture and taste modifier, pharmaceutical excipient, and biomaterial for tissue engineering [23–26].

D. moldavica L., a medicinally valuable perennial herb, is commonly referred to as "Moldavian dragon's head" and categorized within the genus *Dracocephalum* and the family Lamiaceae [27]. The phytochemical investigations of the plant revealed an unparalleled reservoir of phytoconstituents, predominantly including flavonoids, terpenoids, glycosides, phenolic acids, lignans, coumarins, and polysaccharides [28]. Additionally, the plant has a long medical history of treating/preventing various ailments, viz., respiratory congestion, inflammation, tachycardia, bronchitis, neuralgia, headache, and gastric, kidney, and liver disorders [29]. Interestingly, the outer layer of *D. moldavica* seeds yields a translucent, polymeric substance composed of a complex mixture of hydrophilic, highly branched polysaccharides (65.04%), proteins (4.28%), and lipids (8.0%) with

exceptional water-holding capacity and viscosity-building potential [27,30]. Plant-derived mucilaginous materials are emerging ingredients with multifaceted properties such as intrinsic biocompatibility, biodegradability, non-toxicity, stability over a range of concentrations, and non-immunogenic nature, making them promising candidates for biomedical applications [31,32].

Although significant progress has been made in fabricating MnO NPs utilizing plant extracts, the application of mucilage continues to be overlooked. The motivational point of this study was to develop novel MnO NPs by leveraging the phytoconstituents of a biomass-based precursor, i.e., *D. moldavica* seed mucilage, as a natural reducing as well as capping agent, thus minimizing waste generation and mitigating dependence on hazardous reagents. Subsequently, the feasibility of the mucilage to substitute conventional synthesis methods was validated through physicochemical, structural, morphological, and elemental evaluations of the synthesized materials using UV-Vis, FTIR, XRD, SEM, and energy-dispersive X-ray (EDX) techniques.

Materials and methods

Potassium permanganate ($KMnO_4$), as a precursor for Mn^{2+} ions, was a commercial laboratory-grade product, whereas *D. moldavica* seeds containing the bioactive constituents necessary for the biogenic synthesis of MnO NPs were supplied by Zielona Poczta, Poland. Sodium hydroxide (NaOH), used to adjust pH, was procured from Sigma Aldrich, while distilled water was employed in all experimental procedures.

Isolation of *D. moldavica* seed mucilage

D. moldavica seeds were well-rinsed using tap water, followed by multiple washes with distilled water for thorough cleaning and decontamination. The extraction was carried out by rehydrating the washed seeds (seeds: distilled water mass ratio of 1:30) at a designated temperature (50 °C) and pH (8.5) using an electric mixing paddle (450 rpm, 2 h, IKA RW 20 digital). Afterward, the seed-water slurry was agitated (1200 rpm,15 min) to facilitate maximum mucilage release and subsequently filtered using a two-fold organza fabric. The mucilage was recovered from the filtrate via centrifugation (10000 rpm, 8 min, Centrifuge 580R) and finally washed with distilled water thrice. To facilitate preservation, the mucilage was oven-dried (DZ-2BC vacuum oven) at 55 °C for approximately 48 h, converted to a finely ground material using a mechanical grinder (Cloer 7580, Germany), and preserved in a sealed container for analytical evaluation. FIG. 1 represents a schematic diagram of *D. moldavica* seed mucilage extraction.

Bio-fabrication of MnO NPs

To proceed with the biosynthesis of MnO NPs, initially, different concentrations (10, 20, and 30 mM) of $KMnO_4$ solutions were prepared individually in distilled water (10 mL), mixed for 10 min at room temperature with various amounts (0.5, 1.0, and 2.0% in 10 mL distilled water) of *D. moldavica* seed mucilage, and homogenized for a duration of 1 h until complete dissolution was achieved. The resulting reaction mixtures were heated at 60 °C for 2 h under mechanical agitation (550 rpm). A color variation from dark purple to blackish brown suggested the completion of the chemical reduction process. Based on the preliminary procedures, the most effective concentrations included 20 mM $KMnO_4$ solution and 1% mucilage suspension. The colloidal suspension of the prepared NPs was transferred to falcon tubes for centrifugation at 6500 rpm for 10 min, separating the liquid layer and the solid residue. The pellet containing as-produced NPs was then purified thoroughly with distilled water to remove excess salt/mucilage residues, and oven-dried for 5-6 h at 55 °C. After collection, the as-synthesized NPs were calcined at 400 °C for 3 h, powdered, and kept in Eppendorf tubes. The experimental procedure of MnO NPs synthesis utilizing *D. moldavica* seed mucilage is illustrated in FIG. 2.

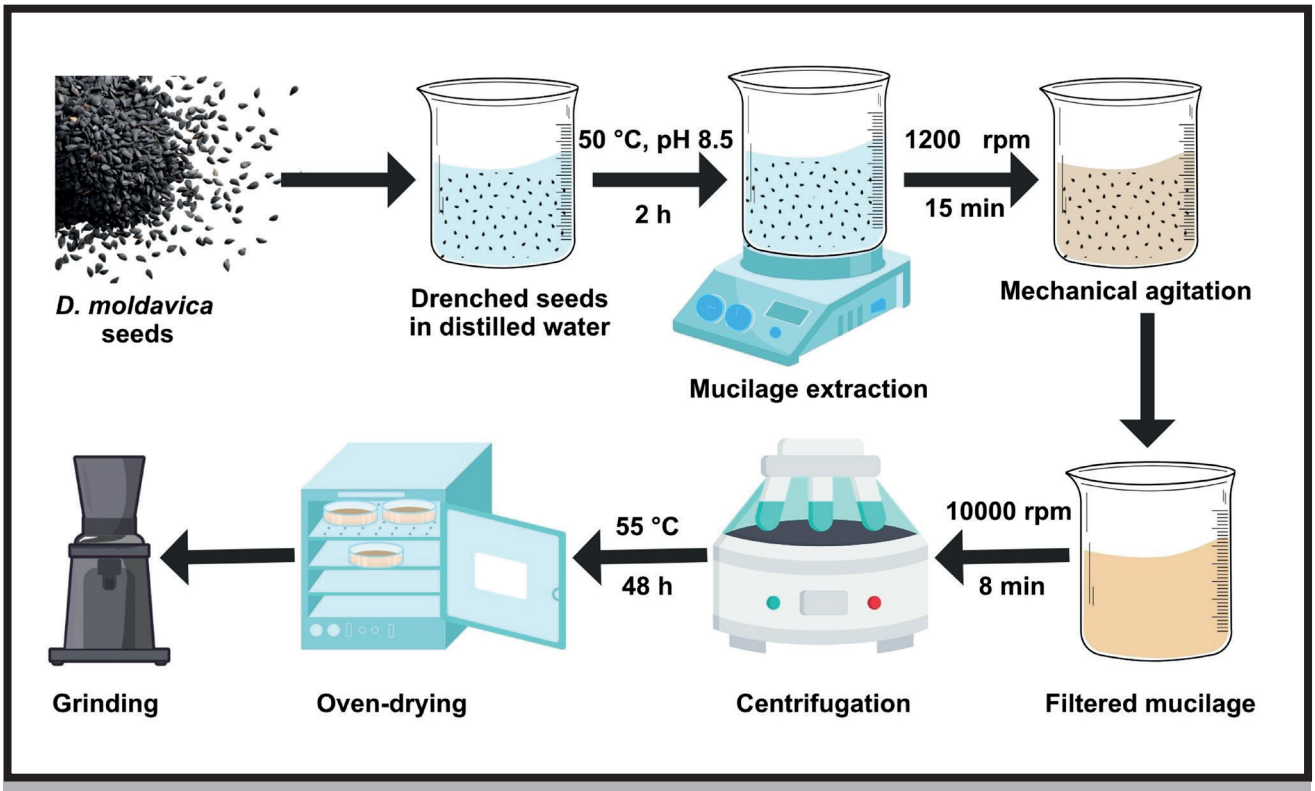


FIG. 1. Protocol for the isolation of *D. moldavica* seed mucilage

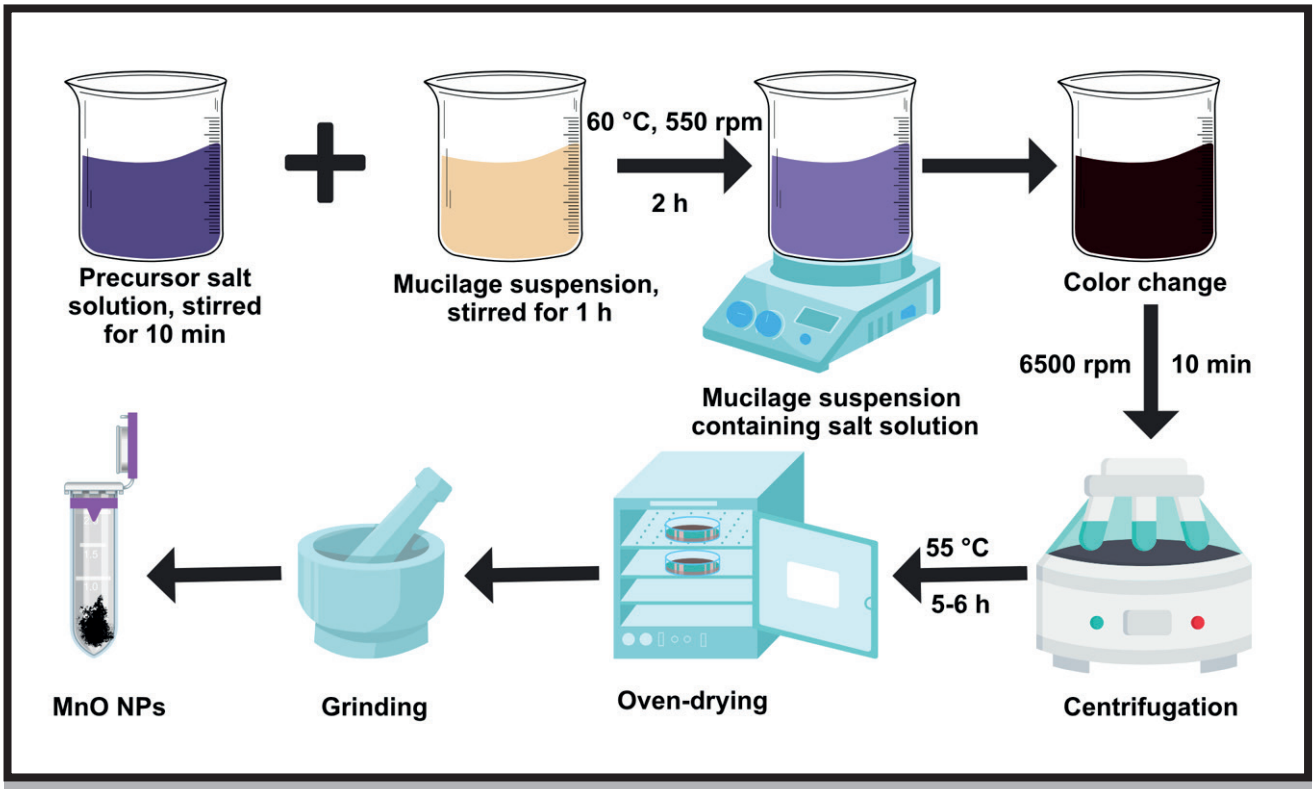


FIG. 2. Step-by-step diagrammatic representation of the biosynthesis of MnO NPs

Characterization

UV-vis spectroscopy

Recently, the UV-Vis spectroscopic method has gained a high interest in the characterization of the NPs, especially after synthesis, as the color of the reaction medium changes, thereby providing valuable evidence regarding the formation and stability of the synthesized materials [33]. In this study, *D. moldavica* seed mucilage-capped MnO NPs (1 mg) were weighed, dispersed in distilled water (10 mL), and exposed to ultrasonic waves (10 min), ensuring uniform distribution of the tested sample. The analysis was performed by placing a quartz cell (3 mL) with an optical path of 1 cm on a SHIMADZU UV-vis spectrophotometer (UV-1601), and the intensity of the transmitted light was measured as a characteristic of the surface plasmonic resonance.

FTIR

FTIR analysis was carried out using a Nicolet iS10 spectrometer (Thermo Fisher Scientific, Waltham, MA, USA) to characterize the surface chemistry and detect diverse organic moieties deposited on the surface of NPs. Before carrying out sample measurement, MnO NPs were integrated with a suitable potassium bromide (KBr) matrix to obtain a compacted thin layer, and spectra for both *D. moldavica* seed mucilage and the biogenic MnO NPs were obtained across the wavelength range of 4000 to 500 cm^{-1}, covering most of the characteristic vibrational frequencies of biomolecules.

XRD

The information regarding the phase composition and crystalline nature of the fabricated material was obtained using a multipurpose diffractometer (Philips X"Pert, with X'Celerator Scientific detector), employing an X-ray source of ceramic copper (Cu Kα, λ=0.15406 nm). Finely powdered MnO NPs were uniformly dispersed onto the sample holder, and the instrument was operated under acceleration voltages and current values of 15-60 kV and 5-55 mA, respectively. The diffraction data, constructive interference of monochromatic X-rays with the crystalline specimen, were patterned throughout the 2θ range of 0-80° at 0.0010/min.

SEM-EDX

Morphology-based examinations of the sample by direct visualization, as well as compositional characteristics, were evaluated using a SEM instrument equipped with an EDX system. To do so, the powdered NPs were mounted on the carbon-coated aluminium stub, sputter-coated with a fine sedimented pellet of conductive metal, and then irradiated with a focused fine beam of electrons at an accelerating voltage of 5-20 kV. The backscattering of the secondary electrons was monitored by the SEM detector (LEO Electron Microscopy Ltd, England, model 1430 VP, 2001), generating images of several regions of the material's surface. At the same time, an energy-dispersive detector (Quantax 200 with XFlash 4010 detector, Bruker AXS, Germany, 2008) was utilized to measure characteristic X-ray emissions, corresponding to the elemental mapping of the synthesized material.

Results and Discussion

Bio-fabrication of MnO NPs

At present, a variety of physicochemical methodologies are being employed to create MnO NPs. However, these traditional techniques frequently call for more than one hazardous reductant/solvent, extreme temperature/pressure conditions, high energy consumption, expensive waste disposal practices, and the technical expertise of well-equipped professionals, thereby highlighting the need for facile, cost-effective, and reproducible approaches [5]. Green-engineered NPs synthesized from bio-resources, such as plants, enzymes, and phytoconstituents, are potentially

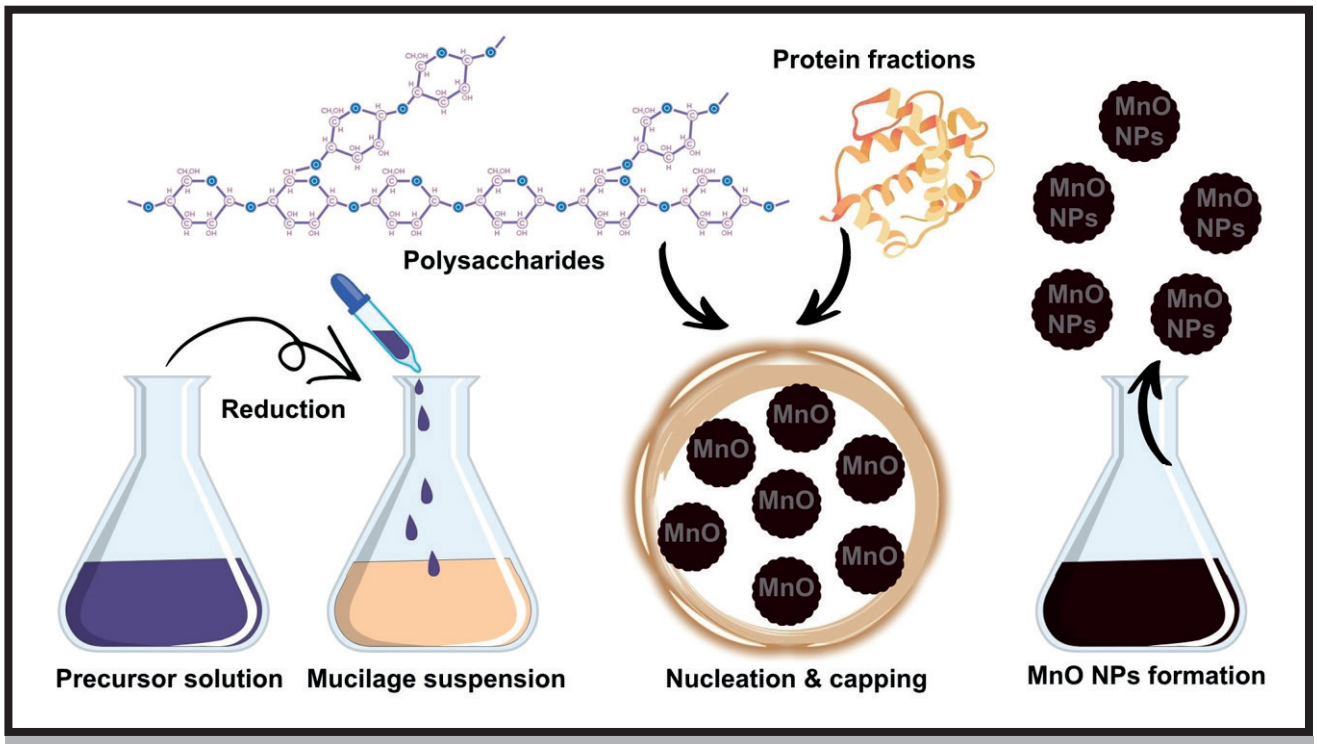


FIG. 3. Proposed mechanistic pathway showing reduction, nucleation, and capping of MnO NPs

advantageous over those generated via conventional approaches, due to their environmental compatibility, economic efficiency, enhanced surface functionality, and reduced cytotoxicity. In the past few years, research regarding the production of nano-MnO using biological macromolecules (particularly mucilage) has gained momentum as an environmentally friendly fuel [34]. Plant-derived mucilage, predominantly comprising anionic polysaccharides covalently bound to proteins, serves a dual role as both a reductant and a stabilizing agent in mediating the fabrication of the NPs [24,25]. Within this context, the viability of *D. moldavica* seed mucilage for reducing a metal precursor ($KMnO_4$) into metal NPs was investigated. A transformation from dark purple to blackish brown color was initially noticed, pointing towards the successful formation of MnO NPs [35]. It is assumed that the polysaccharide network chains/protein fractions of *D. moldavica* seed mucilage might be responsible for the reduction and subsequent production of the NPs. The predicted reaction mechanism underlying the biogenic synthesis of MnO NPs is given in FIG. 3.

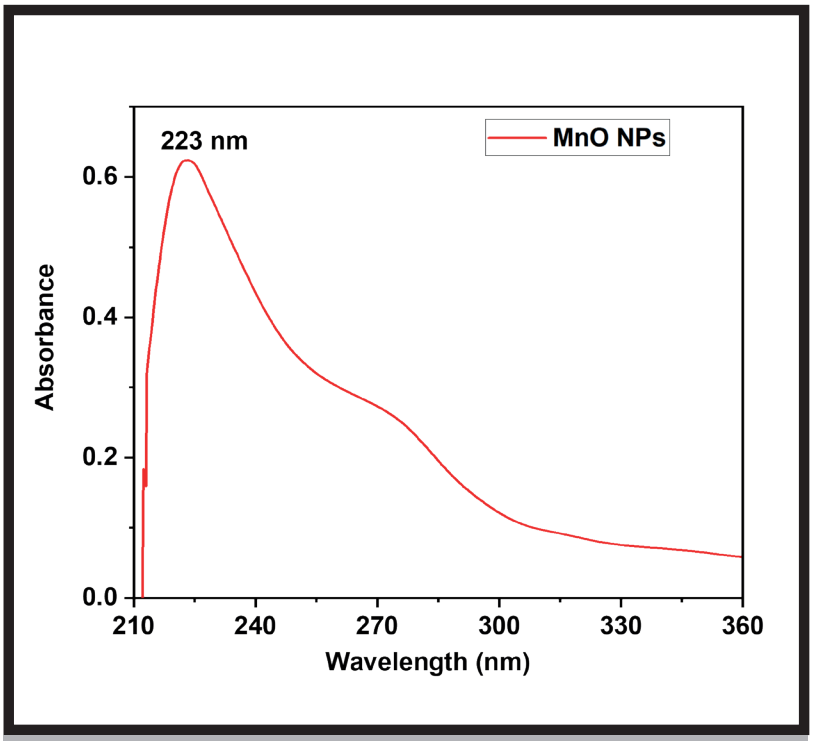


FIG. 4. UV-vis absorption spectrum of the bio-engineered MnO NPs

UV-Vis spectroscopy

Manganese oxide-based NPs have been shown to exhibit a wide range of oxidation states, viz., MnO, MnO_2, Mn_2O_3, Mn_3O_4, and others, which directly impact their optical and physicochemical properties. A UV-vis spectrophotometer can easily monitor distinctive absorption characteristics corresponding to the degree of reduction/oxidation, thus enabling the identification of the predominant state in the nanosuspension [36]. In the present investigation, *D. moldavica* seed mucilage-reduced/cap manganese oxide-based NPs presented a distinguishable SPR peak at around 223 nm (FIG. 4), pertaining to electronic transitions between the conduction and valence bands. Previously, *Dittrichia graveolens* plant extract-synthesized and curcumin-functionalized MnO NPs showed the maximum absorption at 240 nm [37], serving as a clear indicator of the presence of the MnO phase in our sample. On the contrary, MnO NPs produced by the chemical synthesis technique, i.e., co-precipitation, revealed characteristic excitations (328 and 365 nm) above the wavelength range

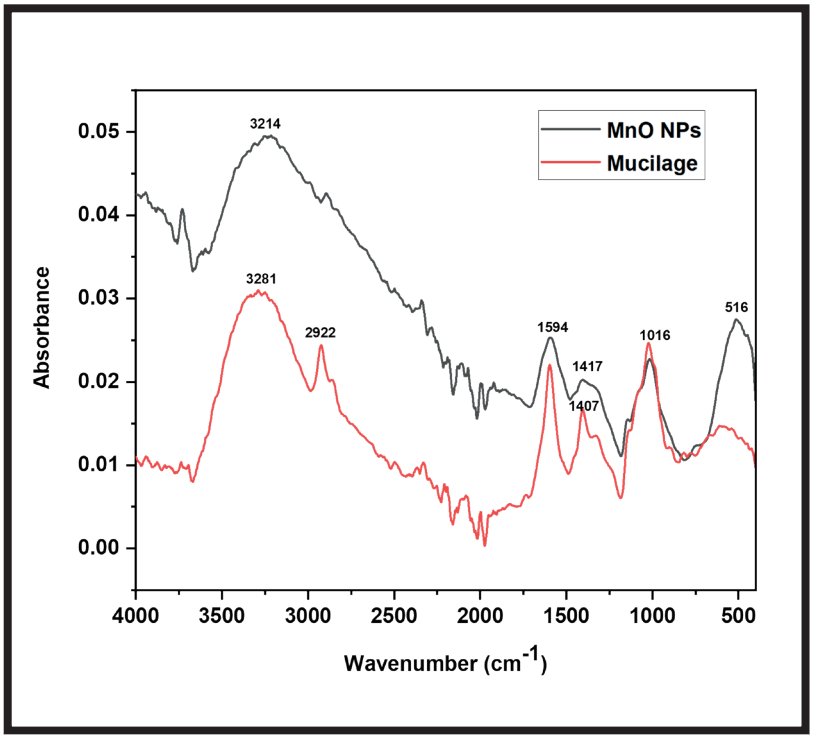


FIG. 5. FTIR spectra of *D. moldavica* seed mucilage and as-fabricated MnO NPs

of their counterparts [38], demonstrating the contribution of the production method in guiding the electronic structure/optical characteristics of the developed materials. The decreased intensity of the absorption peak in the green-synthesized MnO NPs may be due to the mucilage's reducing phytochemicals.

FTIR

The interactions between *D. moldavica* seed mucilage and as-synthesized MnO NPs were investigated using FTIR analysis. The absorption patterns were captured over the spectral range of 4000-500 cm^{-1}, and the results showed several peaks corresponding to different molecular functionalities (FIG. 5). For instance, the carbohydrate moieties of free –OH groups were detected at 3281 cm^{-1}, while the distinctive infrared band appearing at 2922 cm^{-1} corresponded to $–CH_2$ groups [39]. The vibrational band centred at around 1594 cm^{-1} was associated with C=O stretching, whereas the O–H bending vibration was linked to a peak at 1407 cm^{-1}, respectively. Finally, the strong band related to -C-O-C- glycosidic linkage was visible at 1016 cm^{-1} [27], suggesting the involvement of polysaccharides in the reduction/capping mechanism. The FTIR curve of MnO NPs derived from *D. moldavica* seed mucilage displayed an IR band at around 516 cm^{-1} (Mn-O linkage), which matched well with the literature [22,37]. Alternatively, MnO NPs fabricated via hydrothermal reaction of $KMnO_4$ and $MnSO_4$ indicated various peaks at 471, 523, 545, 586, and 718 cm^{-1} [40], unveiling their unique surface chemistry. In general, green-generated MnO NPs differ from their chemically synthesized counterparts in terms of diverse absorption bands, probably because of a wide capping of phytochemicals influencing the chemical environment of the nanomaterial's surface.

X-ray diffraction

The detailed information about the crystallinity of the biogenic MnO nanostructures was assessed using powdered XRD measurements, and the characteristic peaks observed in the angular range of 2θ = 20–80° are illustrated in FIG. 6. The resultant spectrogram confirmed the existence of well-oriented peaks at 22.4, 37.12, and 65.9° corresponding to (211), (101), and (002) planes, thus consistent with the standard diffraction data of PDF#07-0230 and giving confidence in the cubic structure of MnO NPs. Additional peaks in the experimental diffractogram have been identified owing to the precipitation of bioorganic phases present in the vicinity of the NPs. Similar results were found for MnO NPs developed using watermelon seed shell and green tea extracts [41,42]. Conversely, extremely weak peaks were noticed in the XRD spectrum of chemically prepared MnO NPs, clearly indicating the amorphous/highly disordered network of the synthesized structures. However, similar material, when calcined at 600 and 800 °C, showed clearly defined signals with the cryptomelane phase (OMS-2), along with additional peaks corresponding to Mn_2O_3 [43].

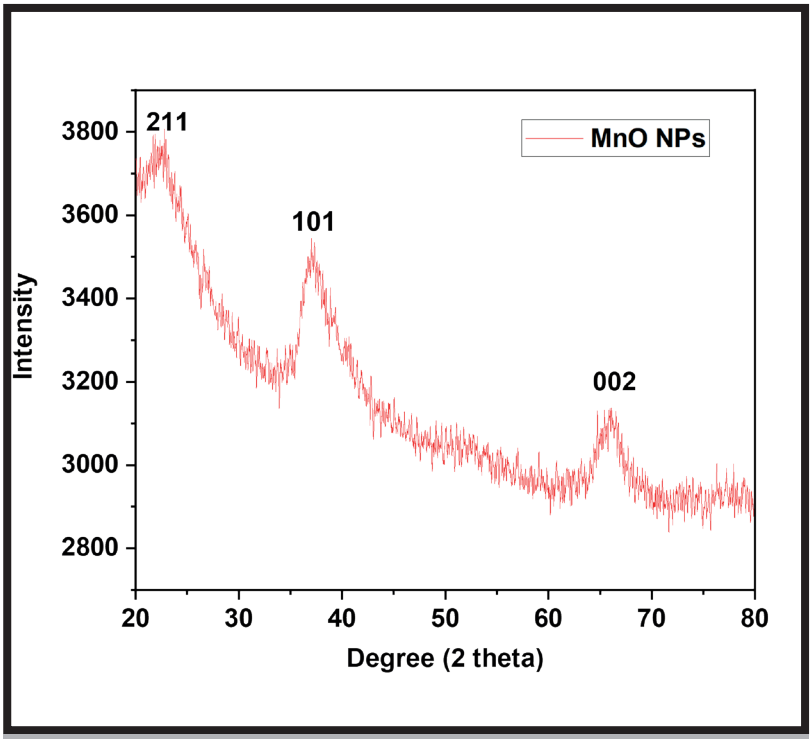


FIG. 6. XRD pattern of *D. moldavica* seed mucilage-reduced/caped MnO NPs

SEM

SEM is one of the most employed methodologies for exploring the microstructure and morphological attributes of nanomaterials, either organic or inorganic. The instrument employs an electron beam with low energy, capturing back-scattered electrons and revealing the surface characteristics of the specimen. According to the SEM observations, *D. moldavica* seed mucilage-mediated MnO NPs predominantly possessed a roughly spherical morphology and a mean size of 82.5 nm. Moreover, NPs appeared anchored on the mucilage's matrix, possibly due to the hydrogen bonding and/or electrostatic interactions between the bioorganic components and the bonds of the atoms making up the material [44]. Some degree of particle aggregation was also observed, attributed to the insufficient involvement of capping agents/weak interactions. The morphological appearance of the NPs observed in this study is analogous to the results obtained by *Jayandran et al.*, where lemon's methanolic extract-reduced and curcumin-stabilized MnO NPs demonstrated spherical morphology with a narrow size distribution (50 nm) [45]. On the other hand, MnO nanostructures synthesized under a basic environment utilizing an ammonia aqueous solution of $KMnO_4$ showed highly dispersed spheres with a diameter of 300 nm [43]. Another study reported the presence of sheet-like massive structures with notable growth and agglomeration in the MnO samples created using the co-precipitation method [38], implying that the green-synthesis route offers a sustainable way to produce particles within the nanoscale range. FIG. 7 provides a detailed depiction of the SEM micrographs of *D. moldavica* seed mucilage-reduced/caped MnO NPs, taken at 1 (a) and 2 μm (b), along with a particle size distribution curve (c).

EDX

The elemental distribution mapping of the biosynthesized MnO NPs was further confirmed by EDX, which measures emitted X-rays and their intensity distributions as indicators of elemental composition and density, respectively. Herein, the EDX analysis, depicted in FIG. 8, shows substantial amounts of manganese (45.07%) and oxygen (41.87%) in the sample, likely due to the formation of MnO NPs.

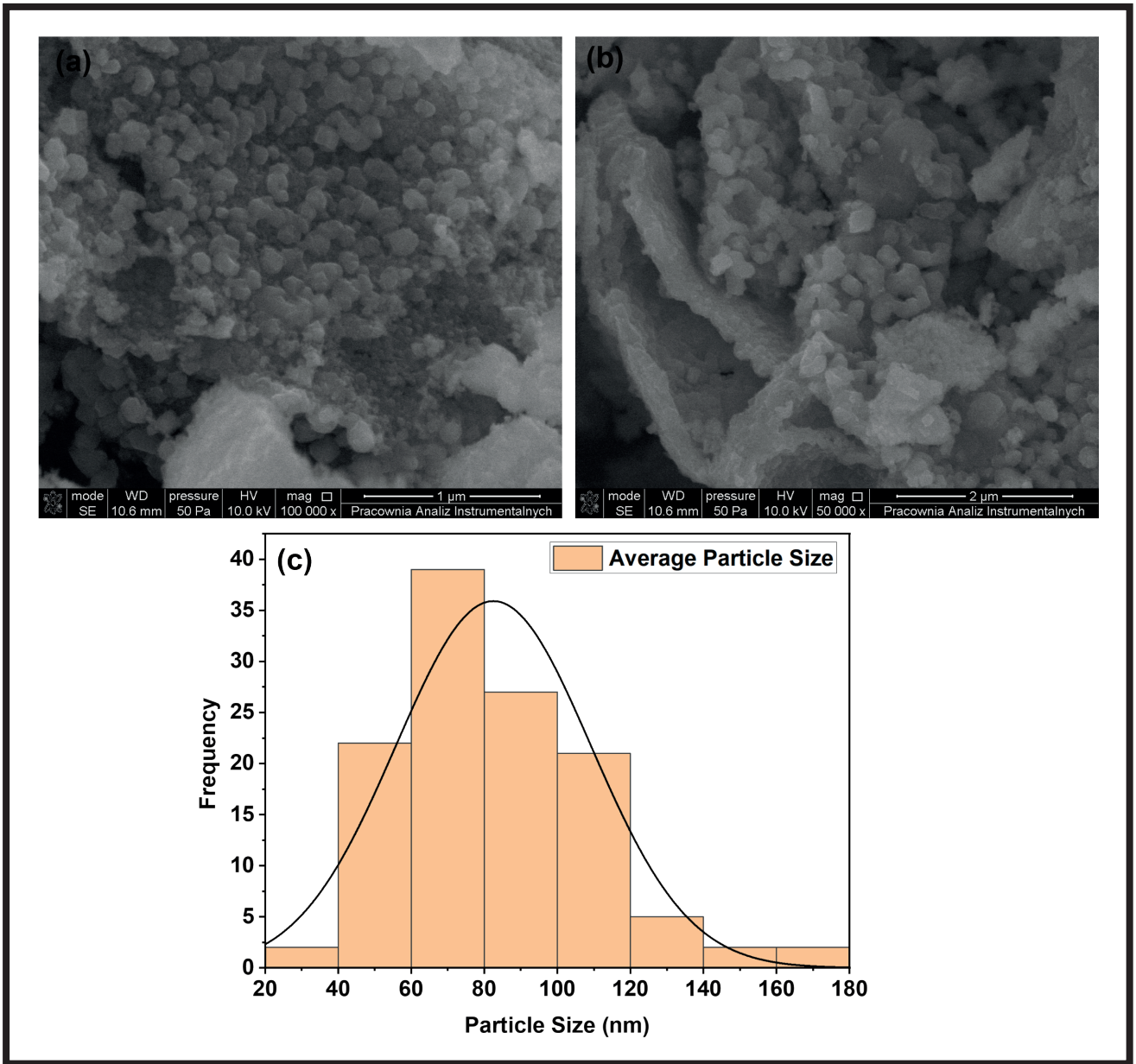


FIG. 7. SEM images of the biogenic MnO NPs (a) and (b), and a particle size distribution histogram (c)

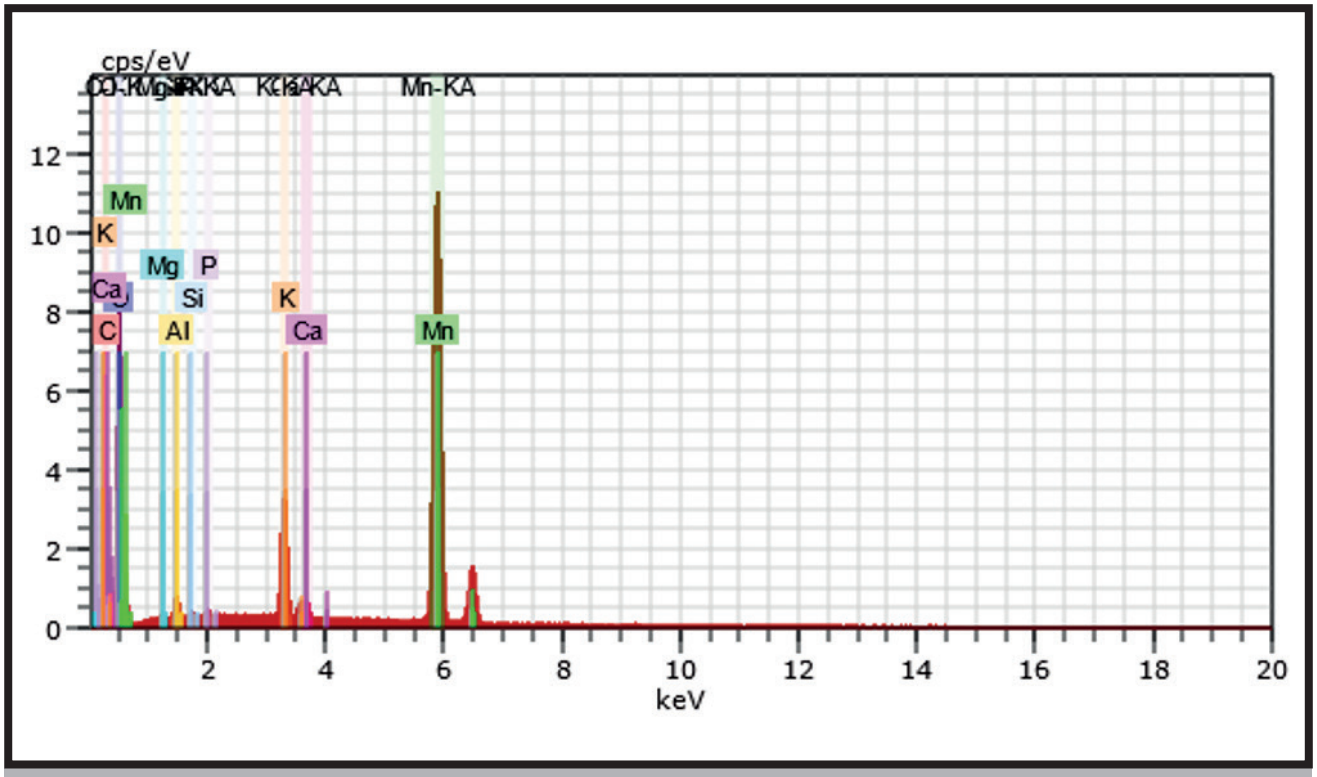


FIG. 8. EDX signals corresponding to mucilage-capped MnO NPs

The spectrum also signified the presence of weak signals related to carbon (4.87%), magnesium (0.23), aluminium (1.04), silicon (0.06), phosphorus (0.18), potassium (5.70), and calcium (0.98), which can be traced to the bioactive substituents in *D. moldavica* seed mucilage covering the NPs' surface. An examination carried out by *Shah et al.* corroborated that the *Albizia procera* leaf extract-synthesized MnO NPs displayed a few inorganic ions (carbon, calcium, and silicon) in the EDX spectrum, apart from the occurrence of manganese and oxygen [46]. Also, the findings of our previous study on the synthesis of MnO NPs using *Cydonia oblonga* seed mucilage revealed multiple signals (carbon, calcium, chlorine, potassium, magnesium, sodium, and silicon) in addition to those attributed to manganese (39.29%) and oxygen (29.3%) [22]. In another case, the EDX pattern indicated the elemental composition of MnO NPs prepared using the chemical technique dependent on NaOH and $MnSO_4$, including manganese, oxygen, silicon, sulfur, copper, and zinc [47], establishing the presence of unwanted residual chemicals/impurities along with the synthesized nanomaterials.

From the above discussion, it is evident that the characteristics of the NPs synthesized using *D. moldavica* seed mucilage are significantly different from their conventional counterparts. These procedures typically generate MnO NPs using expensive and toxic chemical species/molecules under stringent reaction conditions, which could endanger both human health and the environment. However, the approach presented here utilizes an inexpensive and environmentally benign biological source, lowers production cost, and reduces environmental impact, thereby aligning well with the principles of green chemistry. Additionally, mucilage's phytoconstituents acting as capping agents remain attached to the surface of the NPs, which may enhance the biocompatibility/activity of the resulting materials for potential biomedical/environmental applications.

Conclusion

In this study, we have shown a rapid, straightforward, and innovative approach for the biosynthesis of MnO NPs by utilizing *D. moldavica* seed mucilage as a suitable alternative to toxic conventional methods. The formation and properties of as-synthesized NPs were evaluated using a comprehensive suite of analytical techniques, such as UV-Vis and FTIR spectroscopy, XRD, SEM, and EDX. The success of the method was monitored via visual observation through the color change of the reaction mixture, corroborating the hypothesis that the bioactive molecules of *D. moldavica* seed mucilage might have caused the quick reduction of metal ions to their respective NPs. UV-Visible examination of the formulation containing MnO NPs showed a distinct broad peak at 223 nm, whereas the peaks associated with the organic functional groups adsorbed on the NPs' surface were revealed using the FTIR analysis. XRD results indicated broad and low-intensity peaks ascribed to the cubic phase composition, while SEM captured roughly spherical particles with an average grain size of 82.5 nm, falling within the size range of the NPs. The EDX spectrum unveiled that manganese and oxygen, as the principal elements, were present within the analyzed sample with weight percentages of 45.07% and 41.87%, respectively. The findings of this study highlight the significance of biopolymers for NPs synthesis owing to their inherent features of operational simplicity, environmental sustainability, cost-effectiveness, and built-in reducing/capping capacities. In the future, our research group aims to investigate the applications of *D. moldavica*-reduced/caped NPs for antimicrobial activity and wastewater treatment.

Acknowledgement

This work was co-financed by the Polish Ministry of Science and Higher Education under the programme "Excellence Initiative-Research University".

References

[1] A.A. Firoozi, A.A. Firoozi, M.R. Maghami: Transformative Impacts of Nanotechnology on Sustainable Construction: A Comprehensive Review, *Results in Engineering* 26 (2025) 104973. https://doi.org/10.1016/j.rineng.2025.104973.

[2] R. Ahmed, K.H. Manik, M.S. Islam, A. Rhine, J.J. Mim, N. Hossain: Green synthesis methods for nanoparticles: Principles, biological routes, and physicochemical approaches toward sustainable nanotechnology, *Next Materials* 11 (2026) 101929. https://doi.org/10.1016/j.nxmate.2026.101929.

[3] J. Jeevanandam, Y.S. Chan, M.K. Danquah: Biosynthesis of Metal and Metal Oxide Nanoparticles, *ChemBioEng Reviews* 3 (2016) 55-67. https://doi.org/10.1002/cben.201500018.

[4] S. Malehmir, A. Abedini, A. Sobhani-Nasab, R. Eshraghi, M. Akbari, A. Atapour, A.M. Hasan-Abad: A review of biogenic routes for the manufacture of manganese oxide nanostructures and its anti-cancer, drug delivery, anti-bacterial, and bioimaging potentials, *Inorganic Chemistry Communications* 156 (2023) 111306. https://doi.org/10.1016/j.inoche.2023.111306.

[5] V. Hoseinpour, N. Ghaemi: Green synthesis of manganese nanoparticles: Applications and future perspective–A review, Journal of Photochemistry and Photobiology B: *Biology* 189 (2018) 234-243. https://doi.org/10.1016/j.jphotobiol.2018.10.022.

[6] P. Yadav, A. Bhaduri, A. Thakur: Manganese Oxide Nanoparticles: An Insight into Structure, Synthesis, and Applications, *ChemBioEng Reviews* 10 (2023) 510–528. https://doi.org/10.1002/CBEN.202200056.

[7] B.G.S. Raj, A.M. Asiri, A.H. Qusti, J.J. Wu, S. Anandan: Sonochemically synthesized MnO2 nanoparticles as electrode material for supercapacitors, *Ultrasonics Sonochemistry* 21 (2014) 1933-1938. https://doi.org/10.1016/j.ultsonch.2013.11.018.

[8] S. Chou, F. Cheng, J. Chen: Electrodeposition synthesis and electrochemical properties of nanostructured γ-MnO2 films, *Journal of Power Sources* 162 (2006) 727–734. https://doi.org/10.1016/J.JPOWSOUR.2006.06.033.

[9] G. Qiu, H. Huang, S. Dharmarathna, E. Benbow, L. Stafford, S.L. Suib: Hydrothermal Synthesis of Manganese Oxide Nanomaterials and Their Catalytic and Electrochemical Properties, *Chemistry of Materials* 23 (2011) 3892–3901. https://doi.org/10.1021/cm2011692.

[10] W.-Y. Ko, J. Chen, Y.-H. Chen, K.-J. Li: Solvothermal synthesis of shape-controlled manganese oxide materials and their electrochemical capacitive performances, *Journal of Materials Research*, 29 (2014) 107-114. https://doi.org/10.1557/jmr.2013.238.

[11] M.A.B. Siddique, U.H. Bithi, A.N. Ahmed, M.A. Gafur, A.H. Reaz, C.K. Roy, M.M. Islam, S.H. Firoz: Preparation of Manganese Oxide Nanoparticles with Enhanced Capacitive Properties Utilizing Gel Formation Method, *ACS Omega* 7 (2022) 48007–48017. https://doi.org/10.1021/acsomega.2c05872.

[12] A.M. Alotaibi, A.M. Alansi, I. Alade, T.F. Qahtan: Green nanochemistry approaches for the sustainable synthesis of biomedical nanomaterials and their emerging applications, *Advanced Powder Technology* 37 (2026) 105226. https://doi.org/10.1016/j.apt.2026.105226.

[13] A. Arumugam, C. Karthikeyan, A.S. Haja Hameed, K. Gopinath, S. Gowri, V. Karthika: Synthesis of cerium oxide nanoparticles using Gloriosa superba L. leaf extract and their structural, optical and antibacterial properties, *Materials Science and Engineering*: C 49 (2015) 408–415. https://doi.org/10.1016/J.MSEC.2015.01.042.

[14] T. Saif, A. Azam, Tuba, G. Muhammad, M.R. Raza, A. Majeed, M.A. Raza: Quince seed gel-mediated zinc oxide nanoparticles: Synthesis, characterization, drug loading, and antimicrobial evaluation, *Journal of Chemical Research* 49 (2025). https://doi.org/10.1177/17475198251361571.

[15] Tuba, S. Javed, M.R. Raza, M.U. Sharif, A. Majeed, M.A. Hussain, G. Muhammad: Quince (Cydonia oblonga) seed hydrogel-based green synthesis of copper oxide nanoparticles for photocatalytic degradation of methylene blue and methyl orange, *Desalination and Water Treatment* 318 (2024) 100388. https://doi.org/10.1016/J.DWT.2024.100388.

[16] S.E.D. Hassan, A. Fouda, E. Saied, M.M.S. Farag, A.M. Eid, M.G. Barghoth, M.A. Awad, M.F. Hamza, M.F. Awad: Rhizopus oryzae-Mediated Green Synthesis of Magnesium Oxide Nanoparticles (MgO-NPs): A Promising Tool for Antimicrobial, Mosquitocidal Action, and Tanning Effluent Treatment, *Journal of Fungi* 7 (2021) 372. https://doi.org/10.3390/JOF7050372.

[17] S.H. EL-Moslamy, I.S. Yahia, H.Y. Zahran, E.A. Kamoun: Novel biosynthesis of MnO NPs using Mycoendophyte: industrial bioprocessing strategies and scaling-up production with its evaluation as anti-phytopathogenic agents, *Scientific Reports* 13 (2023). https://doi.org/10.1038/S41598-023-28749-Z.

[18] J.D. Oliveira da Silva, H.C. dos Santos, G.S. Bento, J.F.R. Oliveira, A.K. de Souza Abud, I. de F. Gimenez: Green synthesis of manganese dioxide (MnO2) nanoparticles produced with acerola (Malpighia emarginata) leaf extract, *Materials Chemistry and Physics* 315 (2024) 128963. https://doi.org/10.1016/J.MATCHEMPHYS.2024.128963.

[19] M. Souri, V. Hoseinpour, N. Ghaemi, A. Shakeri: Procedure optimization for green synthesis of manganese dioxide nanoparticles by Yucca gloriosa leaf extract, *International Nano Letters* 9 (2019) 73–81. https://doi.org/10.1007/S40089-018-0257-Z/FIGURES/7.

[20] A. Dixit: An analysis of green synthesis of manganese oxide nanoparticles including applications and prospects as anticancer activity (MTT, ROS & MMP), *International Journal of Botany Studies* 6 (2021) 1452-1456.

[21] V. Kumar, K. Singh, S. Panwar, Surinder, K. Mehta: Green synthesis of manganese oxide nanoparticles for the electrochemical sensing of p-nitrophenol, *International Nano Letters* 2017 7:2 7 (2017) 123–131. https://doi.org/10.1007/S40089-017-0205-3.

[22] T. Ayub, G. Muhammad, M.U. Sharif, M.R. Raza, H. Hanif, M. Amin, M.A. Hussain: Glucuronoxylan hemicellulose-based manganese oxide nanoparticles for enhanced bactericidal, wound healing, and photocatalytic potential, *Journal of Applied Biomaterials & Functional Materials* 23 (2025). https://doi.org/10.1177/22808000251328937.

[23] M.A.H. Shiam, M.S. Islam, I. Ahmad, S.S. Haque: A review of plant-derived gums and mucilages: Structural chemistry, film forming properties and application, *Journal of Plastic Film & Sheeting* 41 (2025) 195–237. https://doi.org/10.1177/87560879251316553.

[24] N.U. Rehman, G. Muhammad, Tuba, M.U. Sharif, M.A. Hussain: Green synthesis of silver nanoparticles using Lepidium sativum seed mucilage as a bioreductant/capping agent for efficient antibacterial and photocatalytic activities, *Desalination and Water Treatment* 320 (2024) 100853. https://doi.org/10.1016/J.DWT.2024.100853.

[25] N.U. Rehman, G. Muhammad, M. Wajid, M.A. Hussain, T. Tuba, M.U. Sharif, A. Majeed, Galactomannan-Stabilized Gold Nanoparticles: A Sustainable Nanoplatform for Biomedical and Environmental Applications, *ChemistrySelect* 10 (2025) e02650. https://doi.org/10.1002/SLCT.202502650.

[26] H. Urena-Saborio, E. Alfaro-Viquez, D. Esquivel-Alvarado, S. Madrigal-Carballo, S. Gunasekaran: Electrospun plant mucilage nanofibers as biocompatible scaffolds for cell proliferation, *International Journal of Biological Macromolecules* 115 (2018) 1218–1224. https://doi.org/10.1016/J.IJBIOMAC.2018.04.129.
[27] M. Beigomi, M. Mohsenzadeh, A. Salari: Characterization of a novel biodegradable edible film obtained from Dracocephalum moldavica seed mucilage, *International Journal of Biological Macromolecules* 108 (2018) 874–883. https://doi.org/10.1016/J.IJBIOMAC.2017.10.184.
[28] M. Zhan, M. Ma, M. Mo, Y. Zhang, T. Li, Y. Yang, L. Dong: Dracocephalum moldavica L.: An updated comprehensive review of its botany, traditional uses, phytochemistry, pharmacology, and application aspects, *Fitoterapia* 172 (2024) 105732. https://doi.org/10.1016/j.fitote.2023.105732.
[29] M.R. Morshedloo, M. Amani Machiani, A. Mohammadi, F. Maggi, M.S. Aghdam, H. Mumivand, A. Javanmard: Comparison of drying methods for the extraction of essential oil from dragonhead (Dracocephalum moldavica L., Lamiaceae), *Journal of Essential Oil Research* 33 (2021) 162–170. https://doi.org/10.1080/10412905.2020.1848652.
[30] K. Maghsoudi, R. Partovi, S.A. Samakkhah: Evaluation of the Effect of Dracocephalum moldavica Mucilage and Nanoemulsion of Satureja hortensis Essential Oil Edible Coating on Microbial, Chemical, and Organoleptic Properties of Rainbow Trout Fish Fillet at Refrigerator Temperature, *Food Science & Nutrition* 13 (2025) e70445. https://doi.org/10.1002/FSN3.70445.
[31] G. Goksen, D. Demir, K. Dhama, M. Kumar, P. Shao, F. Xie, N. Echegaray, J.M. Lorenzo: Mucilage polysaccharide as a plant secretion: Potential trends in food and biomedical applications, *International Journal of Biological Macromolecules* 230 (2023) 123146. https://doi.org/10.1016/J.IJBIOMAC.2023.123146.
[32] V.D. Prajapati, G.K. Jani, N.G. Moradiya, N.P. Randeria: Pharmaceutical applications of various natural gums, mucilages and their modified forms, *Carbohydrate Polymers* 92 (2013) 1685-1699. https://doi.org/10.1016/j.carbpol.2012.11.021.
[33] M. Arif, H. Raza, T. Akhter: UV-Vis spectroscopy in the characterization and applications of smart microgels and metal nanoparticle-decorated smart microgels: a critical review, *RSC Advances* 14 (2024) 38120–38134. https://doi.org/10.1039/D4RA07643E.
[34] K. Nagaraja, M. Arunpandian, O.T. Hwan: A facile green synthesis of manganese oxide nanoparticles using gum karaya polymer as a bioreductant for efficient photocatalytic degradation of organic dyes and antibacterial activity, *International Journal of Biological Macromolecules* 273 (2024) 133123. https://doi.org/10.1016/j.ijbiomac.2024.133123.
[35] D. Afonso Delgado, T. del Pino Alemán, J. Trujillo Bueno: The effect of temperature on structural and optical properties of manganese oxide nanoparticles, *Journal of Physics: Conference Series* 1279 (2019) 012004. https://doi.org/10.1088/1742-6596/1279/1/012004.
[36] R. Baitha, A.K. Das, S. Kumar, Monalisa, A. Manash: Green vs. chemical cerium oxide nanoparticles (CeO_2-NPs): Integrated assessment of synthesis pathways, structural properties, ferroelectric behavior, and biomedical applications, *Solid State Communications* 409 (2026) 116309. https://doi.org/10.1016/J.SSC.2025.116309.
[37] M. Souri, V. Hoseinpour, A. Shakeri, N. Ghaemi: Optimisation of green synthesis of MnO nanoparticles via utilising response surface methodology, *IET Nanobiotechnology* 12 (2018) 822–827. https://doi.org/10.1049/IET-NBT.2017.0145.
[38] T. Mounika, S.L. Belagali, K.T. Vadiraj: Manganese oxide nanoparticles synthesis route, characterization and optical properties, *Materialstoday: Proceedings* 75 (2023) 72-76. https://doi.org/10.1016/j.matpr.2022.11.017.
[39] K. Nagaraja, O.T. Hwan: Green synthesis of Multifunctional Zinc oxide Nanoparticles from Cordia myxa gum; and their Catalytic Reduction of Nitrophenol, Anticancer and Antimicrobial Activity, *International Journal of Biological Macromolecules* 253 (2023) 126788. https://doi.org/10.1016/J.IJBIOMAC.2023.126788.
[40] G. Qiu, H. Huang, S. Dharmarathna, E. Benbow, L. Stafford, S.L. Suib: Hydrothermal synthesis of manganese oxide nanomaterials and their catalytic and electrochemical properties, *Chemistry of Materials* 23 (2011) 3892-3901. https://doi.org/10.1021/cm2011692.
[41] A. Ekinci, S. Kutluay, Ö. Şahin, O. Baytar, O. Şahin: Green synthesis of copper oxide and manganese oxide nanoparticles from watermelon seed shell extract for enhanced photocatalytic reduction of methylene blue, *International Journal of Phytoremediation*, 2023 25 (2022) 789–798. https://doi.org/10.1080/15226514.2022.2109588.
[42] W.M. Saod, L.L. Hamid, N.J. Alaallah, A. Ramizy: Biosynthesis and antibacterial activity of manganese oxide nanoparticles prepared by green tea extract, *Biotechnology Reports* 34 (2022) e00729. https://doi.org/10.1016/J.BTRE.2022.E00729.
[43] T. Soejima, K. Nishizawa, R. Isoda: Monodisperse manganese oxide nanoparticles: Synthesis, characterization, and chemical reactivity, *Journal of Colloid and Interface Science* 510 (2018) 272-279. https://doi.org/10.1016/j.jcis.2017.09.082.
[44] M.M. Priya, B.K. Selvi, J.A.J. Paul: Green synthesis of silver nanoparticles from the leaf extracts of Euphorbia hirta and Nerium indicum, *Digest Journal of Nanomaterials and Biostructures* 6 (2011) 869-877.
[45] M. Jayandran, M. Muhamed Haneefa, V. Balasubramanian: Green synthesis and characterization of Manganese nanoparticles using natural plant extracts and its evaluation of antimicrobial activity, *Journal of Applied Pharmaceutical Science* 5 (2015) 105–110. https://doi.org/10.7324/JAPS.2015.501218.
[46] S.S. Shah, M.A. Aziz, A.K. Mohamedkhair, M.A.A. Qasem, A.S. Hakeem, M.K. Nazal, Z.H. Yamani: Preparation and characterization of manganese oxide nanoparticles-coated Albizia procera derived carbon for electrochemical water oxidation, 30 (1979) 16087–16098. *https://doi.org/10.1007/s10854-019-01979-6*.
[47] S. Dhital, S. Pradhan, S. Aryal, P. Neupane, N. Parajuli, M. Tamang, P. Thanait: Synthesis of manganese oxide nanoparticles using co-precipitation method and its antimicrobial activity, *International Journal of New Chemistry* 11 (2024) 243-253. https://doi.org/10.22034/ijnc.2024.2018867.1368.